Sensitivity Gaussian packets

Luděk Klimeš
Department of Geophysics, Faculty of Mathematics and Physics, Charles University, Ke Karlovu 3, 121 16 Praha 2, Czech Republic, http://sw3d.cz/staff/klimes.htm

Summary

Perturbations of elastic moduli and density are decomposed into Gabor functions. A short–duration broad–band incident wavefield with a smooth frequency spectrum is considered. The wavefield scattered by the perturbations is then composed of waves scattered by the individual Gabor functions. The scattered waves are estimated using the first–order Born approximation with the paraxial ray approximation. For a particular source, each Gabor function generates at most a few scattered Gaussian packets propagating in determined directions. Each of these scattered Gaussian packets is sensitive to just a single linear combination of the perturbations of elastic moduli and density corresponding to the Gabor function. This information about the Gabor function is lost if the scattered Gaussian packet does not fall into the aperture covered by the receivers and into the legible frequency band.

Introduction

We study how the perturbations of a generally heterogeneous isotropic or anisotropic structure manifest themselves in the wavefield, and which perturbations can be detected within a limited aperture and a limited frequency band. We consider a smoothly varying heterogeneous generally anisotropic background medium, with an isotropic background medium as a special case. We consider generally anisotropic perturbations of the medium, with isotropic perturbations as a special case. We decompose the perturbations of elastic moduli and density into Gabor functions, and approximate the waves scattered by individual Gabor functions analytically. Refer to Klimeš (2007) for more details.

Gabor representation of medium perturbations

We consider infinitesimally small perturbations $\delta c_{ijkl}(\mathbf{x})$ and $\delta\varrho(\mathbf{x})$ of elastic moduli $c_{ijkl}(\mathbf{x})$ and density $\varrho(\mathbf{x})$. We decompose the perturbations into Gabor functions $g^\alpha(\mathbf{x})$ indexed here by α:

$$\delta c_{ijkl}(\mathbf{x}) = \sum_\alpha c^\alpha_{ijkl}\; g^\alpha(\mathbf{x}) \quad , \qquad \delta\varrho(\mathbf{x}) = \sum_\alpha \varrho^\alpha g^\alpha(\mathbf{x}) \quad ,$$

$$g^\alpha(\mathbf{x}) = \exp[\mathrm{i}\,\mathbf{k}^{\alpha\,\mathrm{T}}(\mathbf{x}-\mathbf{x}^\alpha) - \tfrac{1}{2}(\mathbf{x}-\mathbf{x}^\alpha)^{\mathrm{T}}\mathbf{K}^\alpha(\mathbf{x}-\mathbf{x}^\alpha)] \quad .$$

Gabor functions $g^\alpha(\mathbf{x})$ are centred at various spatial positions $\mathbf{x}^\alpha$ and have various structural wavenumber vectors $\mathbf{k}^\alpha$. The wavefield scattered by the perturbations is then composed of waves $u^\alpha_i(\mathbf{x},t)$ scattered by individual Gabor functions:

$$\delta u_i(\mathbf{x},t) = \sum_\alpha u^\alpha_i(\mathbf{x},t) \quad .$$

Submitted to the *80th Annual Meeting of Society of Exploration Geophysicists*, Denver, USA, October 17–22, 2010.
In: Seismic Waves in Complex 3–D Structures, Report 20 (Department of Geophysics, Charles University, Prague, 2010), pp. 29–34

Figure 1. A single Gabor function $g^\alpha(\mathbf{x})$ centred at point $\mathbf{x}^\alpha$.

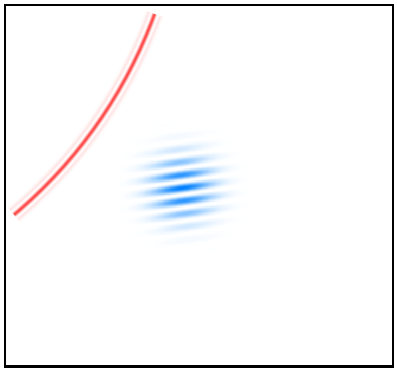

Figure 2. Broad–band wave incident at the Gabor function.

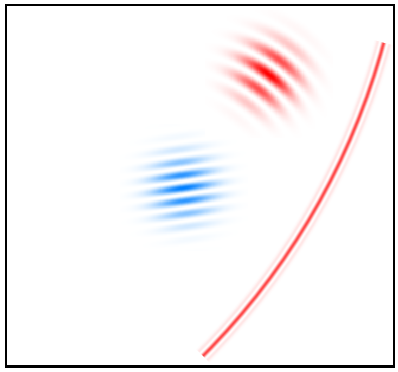

Figure 3. Scattered wave $u_i^\alpha(\mathbf{x},t)$.

Applied approximations

We assume that a short–duration broad–band wavefield with a smooth frequency spectrum, incident at the Gabor function, can be expressed in terms of the amplitude and travel time. We approximate each wave $u_i^\alpha(\mathbf{x},t)$ scattered by one Gabor function by the *first–order Born approximation*, which describes exactly the first–order sensitivity of the wavefield to the infinitesimally small structural perturbations. We apply the *ray–theory approximation* to the Green tensor in the Born approximation. We use the *high–frequency approximation of spatial derivatives* of both the incident wave and the Green tensor. In this high–frequency approximation, we neglect the derivatives of the amplitude, which are of order $1/$*frequency* with respect to the derivatives of the travel time. We make use of the *paraxial ray approximation* of the incident wave in the vicinity of central point $\mathbf{x}^\alpha$ of the Gabor function, and of the *two–point paraxial ray approximation* of the Green tensor at point $\mathbf{x}^\alpha$ and at the receiver. The paraxial ray approximation consists in a constant amplitude and in the second–order Taylor expansion of the travel time. The above mentioned approximations enable us to calculate wave $u_i^\alpha(\mathbf{x},t)$, scattered by the Gabor function, analytically (Klimeš, 2007).

Sensitivity Gaussian packets

Considering the above approximations, wave $u_i^\alpha(\mathbf{x},t)$ scattered by one Gabor function is composed of a few (i.e., 0 to 5 as a rule) Gaussian packets. Each of these "sensitivity" Gaussian packets has a specific frequency and propagates from point $\mathbf{x}^\alpha$ in a specific direction, see Figures 1–3. Each of these sensitivity Gaussian packets scattered by Gabor function $g^\alpha(\mathbf{x})$ is sensitive to just a single linear combination $\sum_{ijkl} c_{ijkl}^\alpha\, E_i\, P_j\, e_k\, p_l - \varrho^\alpha \sum_i E_i\, e_i$ of perturbation coefficients c_{ijkl}^α and ϱ^α corresponding to the Gabor function. Here P_i and E_i are the slowness vector and the unit polarization vector of the incident wave, and p_i and e_i are the slowness vector and the unit polarization vector of the sensitivity Gaussian packet. This information about the Gabor function is lost if the sensitivity Gaussian packet does not fall into the aperture covered by the receivers and into the legible frequency band. The situation improves with the increasing number of differently positioned sources. If we have many sources, the sensitivity Gaussian packets propagating from a Gabor function may be lost during the measurement corresponding to one source, but recorded during the measurement corresponding to another, differently positioned source. However, the problem is not only to record the Gaussian packets from a Gabor function, but to record them in as many different measurement configurations as to resolve perturbation coefficients c_{ijkl}^α and ϱ^α.

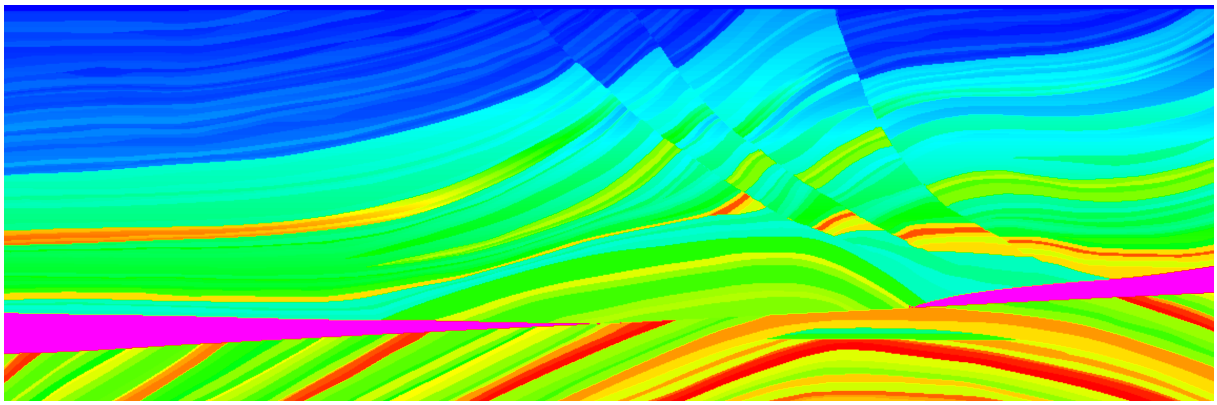

Figure 4. P–wave velocity in the Marmousi structure.

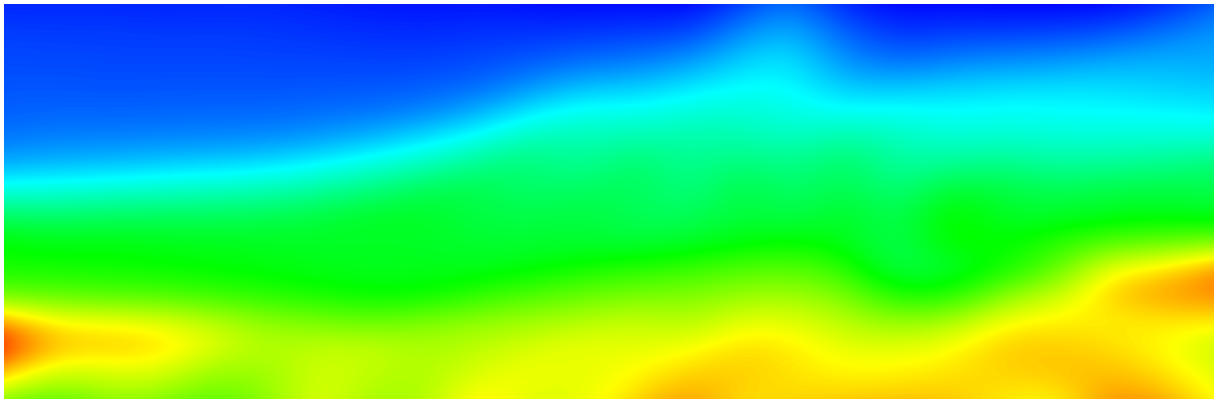

Figure 5. P–wave velocity in the velocity model for ray tracing.

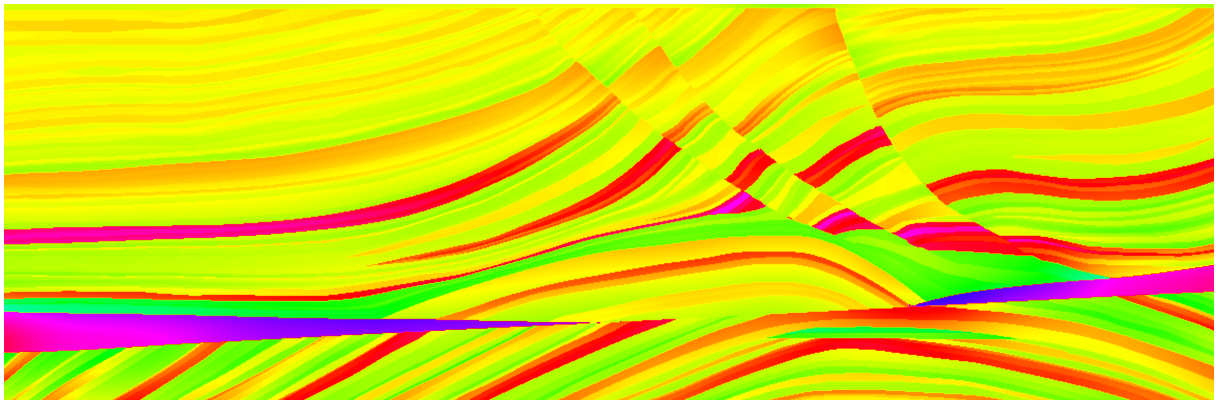

Figure 6. Velocity difference between the Marmousi structure and the velocity model.

Marmousi example

We consider the distribution of the P–wave velocity in the Marmousi structure, see Figure 4. The velocity model for ray tracing must be smooth and is displayed in Figure 5. The velocity difference between the Marmousi structure and the velocity model is displayed in Figure 6.

For the decomposition of the velocity difference, we generate the set of Gabor functions $g^\alpha(\mathbf{x})$ with matrices $\mathbf{K}^\alpha$ optimized according to Klimeš (2008b). We obtain 67014 Gabor functions within the selected wavenumber domain. Refer to Figure 7 for 14 selected Gabor functions. We then decompose the velocity difference from Figure 6 into

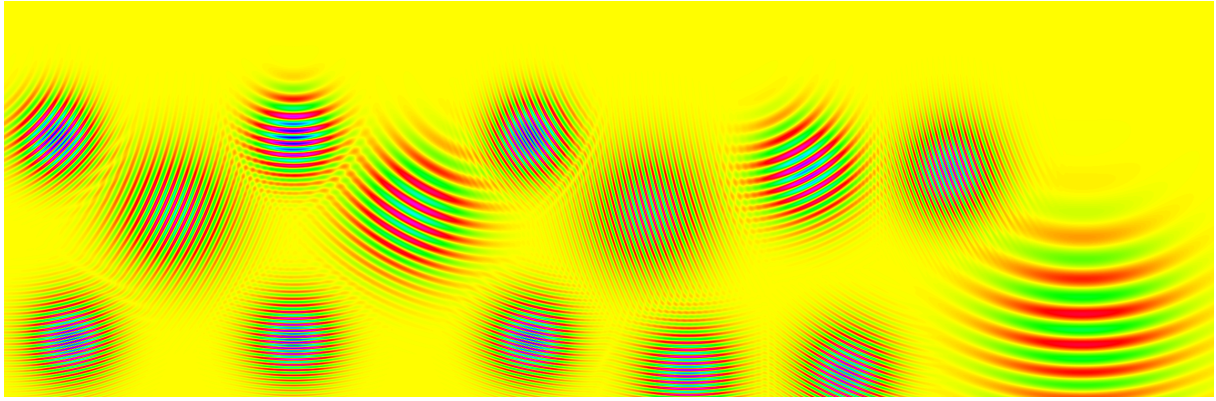

Figure 7. Example showing 14 ones of 67014 optimized Gabor functions used to decompose the velocity difference.

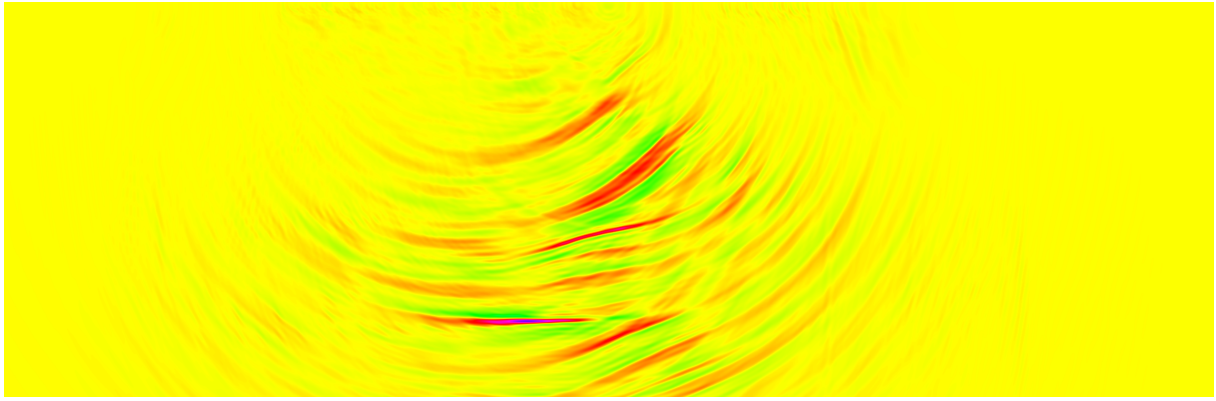

Figure 8. Sum of the Gabor functions influencing the seismograms recorded for shot 70.

the sum of Gabor functions. For each shot, we calculate the quantities describing the paraxial approximation of the incident P wave at all central points of Gabor functions. For each shot and each Gabor function, we calculate the initial conditions for the corresponding sensitivity Gaussian packets which form the scattered wave. We consider Gaussian packets corresponding to the given frequency band only. We then trace the central ray of each sensitivity Gaussian packet. If a sensitivity Gaussian packet arrives to the receiver array within the registration time, the recorded wavefield contains information on the corresponding Gabor function. The sum of the Gabor functions influencing the seismograms recorded for shot 70 is displayed in Figure 8.

The velocity difference from Figure 6 can be decomposed into the part to which the recorded seismograms are not sensitive and into the part to which the recorded seismograms are sensitive. The sum of the Gabor functions influencing the seismograms collected from all shots is displayed in Figure 9. This is the part of the velocity difference to which the recorded seismograms are sensitive. The remaining part of the velocity difference, influencing no recorded seismogram within the first–order Born approximation, is displayed in Figure 10. This part of the velocity difference cannot be recovered from the Marmousi seismograms.

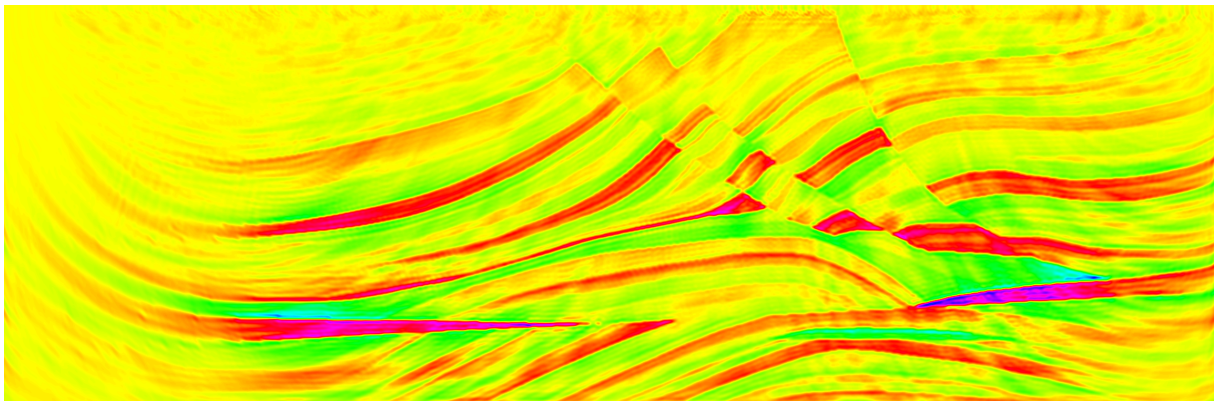

Figure 9. Sum of the Gabor functions influencing the seismograms collected from all shots.

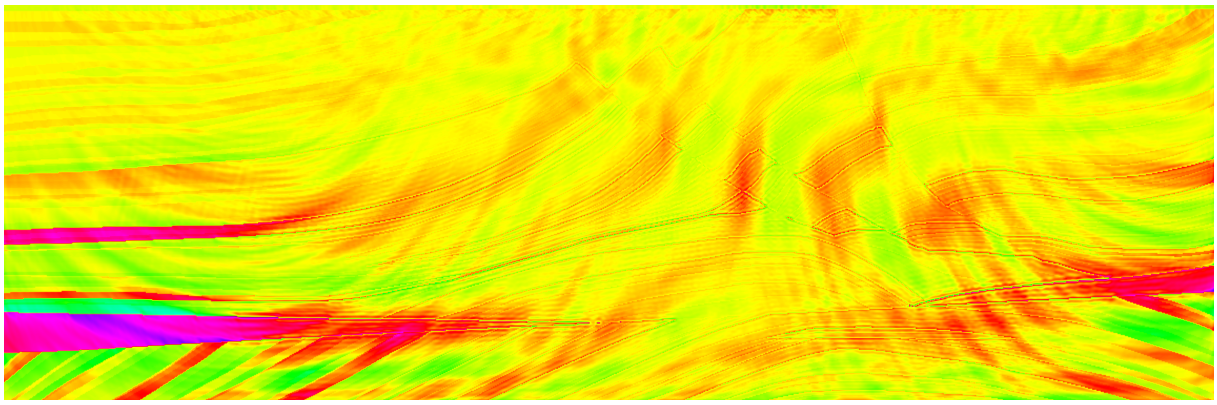

Figure 10. Part of the velocity difference from Figure 6 influencing no recorded seismogram.

Conclusions

Perturbations of elastic moduli and density can be decomposed into Gabor functions. A short–duration broad–band wave with a smooth frequency spectrum incident at each Gabor function generates at most a few scattered Gaussian packets. Each Gaussian packet has a specific frequency and propagates in a specific direction. Refer to Klimeš (2007) for the relevant equations. Each Gaussian packet is sensitive to a single linear combination of the perturbations of elastic moduli and density corresponding to the Gabor function. This information about the Gabor function is lost if the Gaussian packet does not fall into the aperture covered by the receivers and into the legible frequency band.

The sensitivity Gaussian packets can enable to replace migrations by true linearized inversion of reflection seismic data. For the algorithm of the linearized inversion of the complete set of seismograms recorded for all shots refer to Klimeš (2008a).

Acknowledgements

The research has been supported by the Grant Agency of the Czech Republic under contracts 205/07/0032 and P210/10/0736, by the Ministry of Education of the Czech Republic within research project MSM0021620860, and by the members of the consortium "Seismic Waves in Complex 3–D Structures" (see "http://sw3d.cz").

References

Klimeš, L. (2007): Sensitivity of seismic waves to the structure. In: *Seismic Waves in Complex 3–D Structures, Report 17*, pp. 27–61, Dep. Geophys., Charles Univ., Prague, online at "http://sw3d.cz".

Klimeš, L. (2008a): Stochastic wavefield inversion using the sensitivity Gaussian packets. In: *Seismic Waves in Complex 3–D Structures, Report 18*, pp. 71–85, Dep. Geophys., Charles Univ., Prague, online at "http://sw3d.cz".

Klimeš, L. (2008b): Optimization of the structural Gabor functions in a homogeneous velocity model for a zero–offset surface seismic reflection survey. In: *Seismic Waves in Complex 3–D Structures, Report 18*, pp. 115–127, Dep. Geophys., Charles Univ., Prague, online at "http://sw3d.cz".